Low-energy electron scattering by formic acid

C. S. Trevisan,[1] A. E. Orel,[1] and T. N. Rescigno[2]
[1]*Department of Applied Science, University of California, Davis, California 95616, USA*
[2]*Chemical Sciences, Lawrence Berkeley National Laboratory, Berkeley, California 94720, USA*
(Received 31 July 2006; published 17 October 2006)

We report the results of fixed-nuclei complex Kohn variational calculations of elastic electron scattering by formic acid, HCOOH. Momentum transfer and angular differential cross sections for incident electron energies ranging from 0.1 to 15 eV are presented and compared to available experimental data. The low-energy behavior of the cross section is analyzed and found to be consistent with the existence of a virtual state.

DOI: 10.1103/PhysRevA.74.042716 PACS number(s): 34.80.Gs

I. INTRODUCTION

Low-energy electron collisions initiate and drive much of the relevant chemistry associated with radiation damage in biomolecules. Although traditional thinking attributed radiation damage of biological molecules to high-energy primary ionizing radiation events, recent experiments of Sanche and collaborators [1,2] have shown that it is the numerous low-energy secondary electrons produced by the primary ionizing radiation energy that play a key role in causing single and double strand breaks in DNA, especially at energies well below ionization thresholds. This has led to renewed interest in the collision of low-energy electrons with biomolecules, since resonant collisions may be an important mechanism in radiation damage of biological systems.

Formic acid (HCOOH), the simplest organic acid, is of interest in both biological and astronomical environments. In the 1980s, dense clumps of formic acid were found in hot interstellar molecular cores [3,4]. Formic acid is also believed to be important in the formation of biological molecules such as acetic acid and glycine, the simplest amino acid, both of which have also been observed in space. The connection between formic acid and more complex biologically important molecules makes the electron-formic acid system relevant not only to astronomy, but also to numerous biological applications.

Much of the experimental work on formic acid has concentrated on measurements of dissociative electron attachment (DEA) to formic acid [5–7]. These experiments show a strong peak in the DEA spectrum near 1.3 eV incident electron energy, with a width of ~0.5 eV, which correlates with the production of formate ($HCOO^-$) anions. Interestingly, the experiments indicate that as a function of incident electron energy, DEA proceeds with an almost vertical onset that is close to the thermodynamic threshold for the process and also gives some indication of fine structure oscillations on the high-energy tail of the peak. Similar structure had been observed in earlier electron transmission experiments [8,9] and there is also evidence that resonance structure is present in both the elastic [10] and the electron impact vibrational excitation cross sections [11] for this molecule in the 1.5–2.0 eV energy range.

Recently, attention has begun to focus on the determination of absolute scattering cross sections. Two experiments have been published that have concentrated on differential and vibrational excitation cross sections. Vizcaino *et al.* [12] studied elastic electron scattering from formic acid using a crossed-beam electron spectrometer. They measured absolute differential cross sections by employing the relative flow technique, where flow rates for HCOOH and a reference gas (He) are measured at a number of temperatures. This data was used to derive momentum transfer cross sections. Allan [11] carried out high-resolution electron energy-loss experiments and reported absolute differential elastic and vibrational excitation cross sections at 135° from threshold to 5 eV. This experiment showed that the π^* resonance causes strong vibrational excitation as well as serves as the precursor to dissociate attachment.

On the theoretical side, Gianturco and Lucchese [13] carried out a search for negative ion resonances at the equilibrium molecular geometry, using a local potential model. Their calculations gave a π^* shape resonance near 3.5 eV, which they claimed was the probable precursor state for the metastable anion which dissociates to the experimentally observed fragments. Differential elastic cross sections from these authors, cited by Vizcaino *et al.* [12], have also recently appeared [14].

In a previous paper [15], we explained the mechanism for low-energy electron attachment to formic acid. Using first-principles electron scattering calculations, we identified the responsible negative ion state as a transient π^* anion. We pointed out that symmetry considerations dictate that the associated dissociation dynamics must be intrinsically polyatomic: since the anion is forbidden from dissociating to the observed fragments in planar geometry, it must first deform to nonplanar geometries before fragmenting. A second anion surface, connected to the π^* surface through a conical intersection, is involved in the dynamics. This second anion state produced no resonance features in the fixed-nuclei calculations, and was postulated to be a virtual state.

In the present investigation, we report *ab initio* elastic differential and momentum transfer cross sections of low-energy electron scattering from formic acid obtained by employing the complex Kohn variational method. We also present evidence, obtained from the low-energy behavior of the cross section and its dependence on target geometry, to support our earlier claim [15] that there must necessarily exist a virtual state in this system.

In the following section we briefly outline the computational methods used in the present study. Section III presents

TABLE I. Optimized geometry for the neutral ground state of *trans* formic acid. Coordinates are in atomic units, where $a_o = 5.291\,772\,1 \times 10^{-11}$ m is the Bohr radius.

Atomic center	$x(a_o)$	$y(a_o)$	$z(a_o)$
C	0.000000	0.000000	0.000000
O	0.775100	0.000000	2.091570
O	1.428910	0.000000	−2.050200
H	−1.984090	0.000000	−0.504453
H	3.154391	0.000000	−1.558650

our results and compares them to available experimental measurements. We conclude with a brief summary.

II. THEORY

We performed fixed-nuclei scattering calculations using the complex Kohn method. The complex Kohn method is a variational technique which uses a trial wave function that is expanded in terms of square-integrable (Cartesian Gaussian) and continuum basis functions that incorporate the correct asymptotic boundary conditions. Detailed descriptions of the method can be found in previous publications [16,17] and will not be repeated here.

The square-integrable basis set we used was the triple-zeta contraction of the $[9s,5p,1d]$ oxygen and carbon Gaussian basis functions of Dunning [18] centered at each atom, augmented with an additional diffuse p-function ($\alpha = 0.059$) on the oxygens. For the hydrogens, we used Dunning's $[4s,1p]$ Gaussian basis set, again centered at each atom. The variational trial scattering function included numerically generated continuum basis functions, up to and including $l = |m| = 5$.

Formic acid is a planar molecule belonging to the point group C_s. It has two stable forms, the *cis* and the *trans* conformers, determined by the position of the hydrogens relative to the C–O bond. The *trans* conformer is lower in energy by 0.169 eV [19] and is ≈1000 times more abundant at room temperature. Therefore all calculations were carried out for this conformer. The equilibrium geometry of *trans* HCOOH was optimized at the self-consistent field (SCF) level and the nuclear coordinates resulting from this optimization are given in Table I. Our calculations give a value of ∼−0.678 a.u. for the dipole moment, which is somewhat larger than the experimental value of 0.555 a.u. Note that the coordinate system used in Table I and in the calculation was chosen so that the dipole moment lies along the z-axis.

The target molecule was described by a SCF wave function and target response (short-range correlation and long-range polarization) was accounted for by including in the Kohn trial function $(N+1)$-electron terms generated by singly exciting the occupied target orbitals into a space of unoccupied orbitals [20,21]. The latter were chosen by the so-called improved virtual orbital (IVO) procedure [22], in which the virtual orbitals are obtained by diagonalizing a V_{N-1} Fock operator in the subspace of SCF unoccupied orbitals. The $(N+1)$-electron terms included in the Kohn trial function were then obtained by singly exciting all but the three occupied core orbitals (carbon and oxygen $1s$) into all IVO orbitals whose orbital energies were less than 2 hartrees. This procedure gave a spherically averaged polarizability of 18.58 atomic units for the target, compared to the value of ≈22.5 atomic units cited by Vizcaino *et al.* [12], and generated a total (i.e., including both $^2A'$ and $^2A''$ symmetries) of ∼9200 terms in the Kohn trial function.

For electronically elastic scattering by a molecule such as HCOOH that has a permanent dipole moment, the fixed-nuclei treatment must be modified to handle the long-range electron-dipole interaction that dominates the scattering at low energies. To address this problem, we use a hybrid treatment in which only the low order partial-wave components of the fixed-nuclei T-matrix are computed variationally while the higher order terms are included in the Born approximation via a closure formula. Basically, we begin with the exact T-matrix and then add and subtract the T-matrix for a fixed point dipole in the Born approximation:

$$\langle \mathbf{k}'|T|\mathbf{k}\rangle = \langle \mathbf{k}'|T^{Born}|\mathbf{k}\rangle + \sum_{lml'm'} i^{l-l'} Y^*_{l'm'}(\hat{\mathbf{k}}') Y^*_{l'm'}(\hat{\mathbf{k}})(T_{lml'm'} - T^{Born}_{lml'm'}), \quad (1)$$

where the first and last terms are, respectively, the full Born T-matrix for the dipole potential (which can be evaluated in closed form) and its partial-wave expansion. Cross sections are obtained from the T-matrix by averaging over all orientations of the target molecule. The essential point to note is that it is only the difference between the exact and Born T-matrices that is expanded in partial waves and this difference converges very rapidly since higher-order partial wave components of the scattered wave function do not penetrate the molecular core and are not sensitive to the dynamic approximation used to treat them. On the other hand, a partial-wave expansion of the full T-matrix in the fixed-nuclei approximation is formally nonconvergent at all scattering angles. Further details about the treatment of polar targets can be found in [23,24] and references therein.

III. RESULTS

We begin with a presentation of integral cross sections. For polar molecules, the fixed-nuclei approximation we use gives differential elastic cross sections (DCS) that diverge at zero scattering angle and, consequently, infinite total scattering cross sections. This is an intrinsic property of the fixed dipole potential and can only be remedied by explicitly including the rotational motion of the target. Total cross sections are nevertheless often presented by extrapolating the DCS to finite values at zero scattering angle or by employing a truncated partial-wave expansion. Both procedures are somewhat arbitrary. When proper account is taken of the rotational motion [23,24], the total cross sections will depend on the initial rotational state of the target and can be sensitive to the details of the representation of the rotational states employed. On the other hand, when Born-closure is included in the fixed-nuclei treatment, it is perfectly adequate for treating differential scattering out of the forward direction

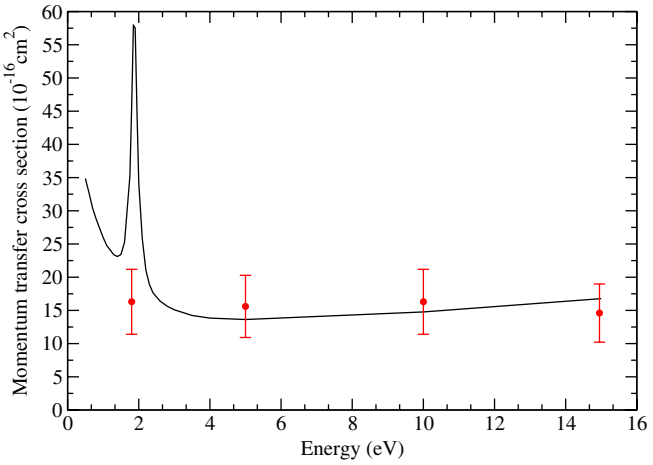

FIG. 1. (Color online) Electron scattering from formic acid: momentum transfer cross sections. Cross sections are in units of 10^{-16} cm^2/sr. Energies are in units of eV = 1.602 176 5 × 10^{-19} J.

and therefore for calculating momentum transfer cross sections (MTCS), which are insensitive to the form of the DCS near 0°. Moreover, since the MTCS is not dominated by the dipole interaction, it can display resonance features more prominently than the total cross section. Figure 1 shows our calculated MTCS, along with the recent measurements of Vizcaino *et al.* [12].

There are two prominent characteristics of the calculated MTCS that are worth commenting on. One is the sharp resonance feature near 1.9 eV, which is the π^* resonance we have recently [15] studied, and the other is the rapid rise in the cross section at lower energies. We note that the calculated cross sections generally fall within the error bars of the measurements, except for the measured value at 1.8 eV, which shows no evidence of a resonance. It is curious that the π^* resonance, which figures so prominently in the calculations, does not leave a strong signature on the vibrationally elastic cross section. This fact is reinforced by the recent measurements of Allan [11] (with which we compare our

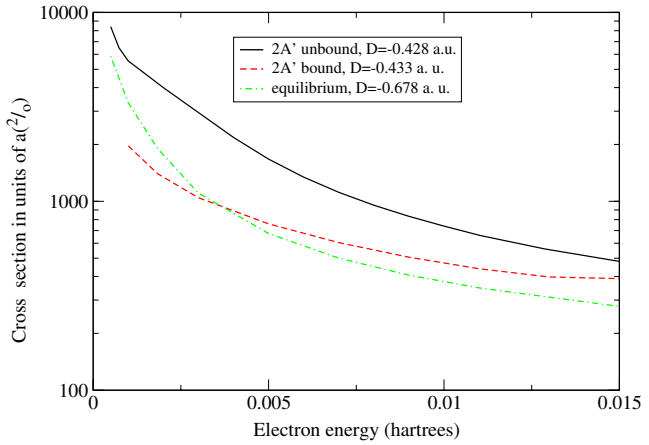

FIG. 2. (Color online) Electron scattering from formic acid: low-energy behavior of cross section for several geometries. Cross sections are in units of 10^{-16} cm^2/sr. Energies are in units of eV. (See text for description.)

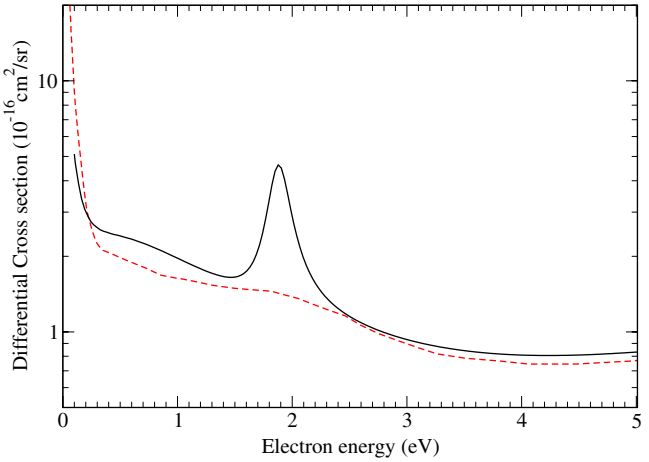

FIG. 3. (Color online) Electron scattering from formic acid: energy dependence of differential cross section at 135°. Solid curve: complex Kohn calculations; and dash curve: experimental data of Allan [11]. Differential cross sections are in units of 10^{-16} cm^2/sr and energies are in eV.

results below), who reports the vibrationally elastic cross section at 135° on a fine energy scale from 0.05 to 5.0 eV. The cross section dips slightly between 2.0 and 4.0 eV, but displays none of the prominent structure seen in the vibrational excitation [11] or dissociative attachment cross sections [7], or in the total transmitted electron current [8,9]. While fixed-nuclei calculations at a single geometry often give resonant cross sections that are larger and narrower than experiment, we would not expect averaging over nuclear geometry to wash out the resonance feature completely. Indeed, we believe that it is more likely that the π^* resonance, once excited, has a relatively small branching ratio to the vibrationally elastic channel, coupling more strongly to the vibra-

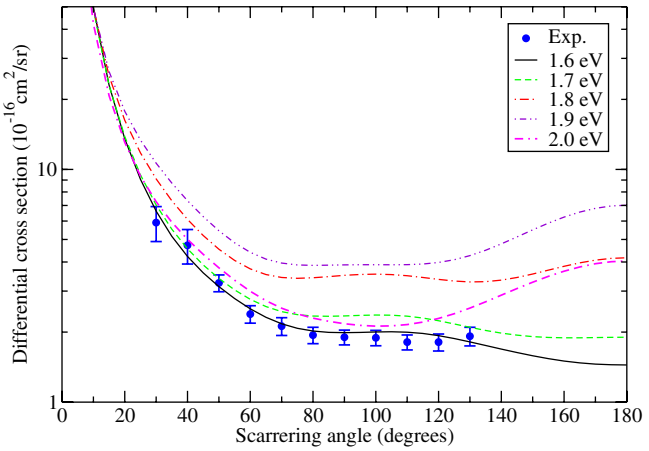

FIG. 4. (Color online) Electron scattering from formic acid: angular differential cross sections. Circles with error bars: experimental data of Vizcaino *et al.* [12] at an incident electron energy of 1.8 eV. Solid curve: complex Kohn calculations at 1.6 eV. Dash curve: complex Kohn calculations at 1.7 eV. Dash-dot curve: complex Kohn calculations at 1.8 eV. Dash-double dot curve: complex Kohn calculations at 1.9 eV. Double dash-dot curve: complex Kohn calculations at 2.0 eV. Differential cross sections are in units of 10^{-16} cm^2/sr and energies are in eV.

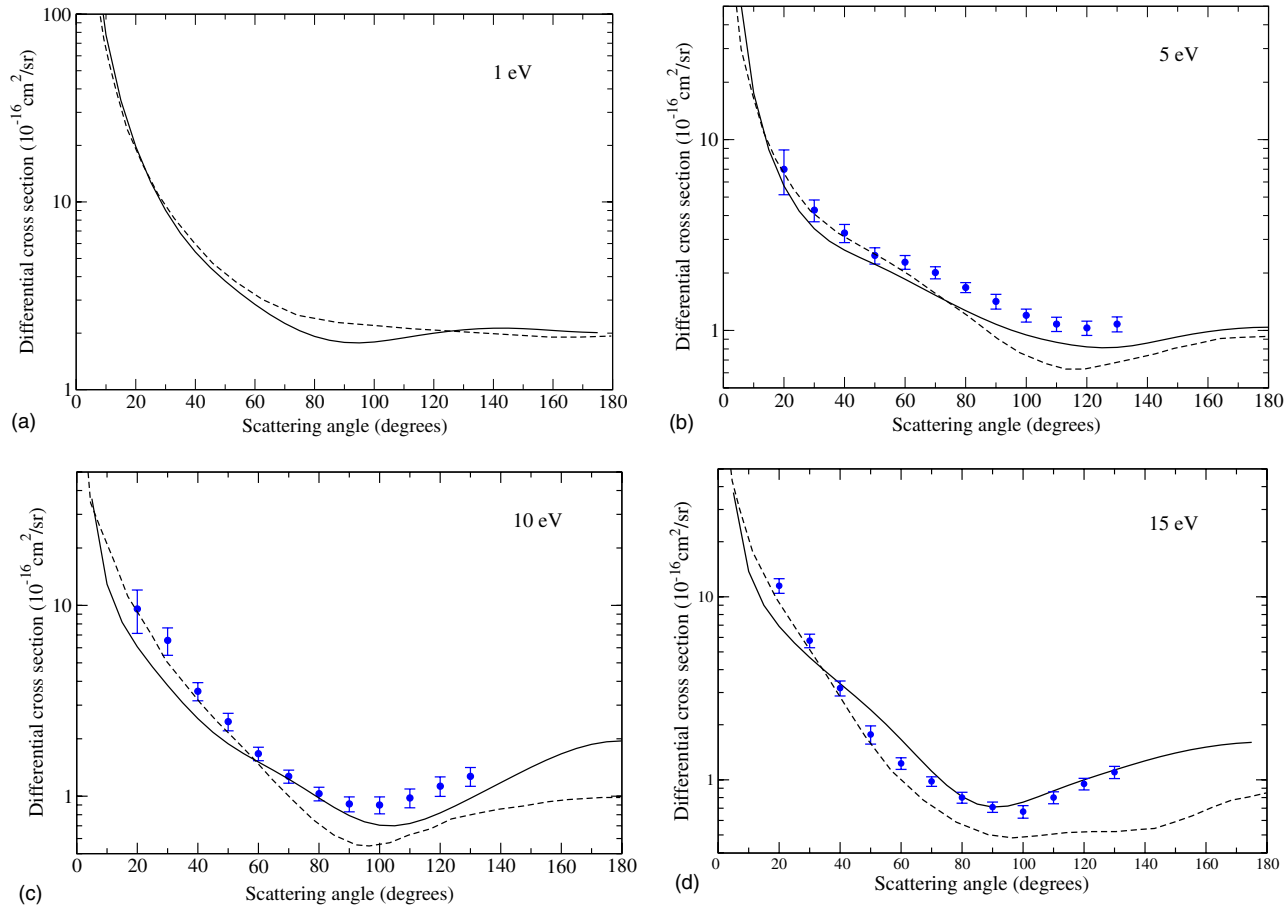

FIG. 5. (Color online) Electron scattering from formic acid: angular differential cross sections for different incident electron energies. Circles with error bars: experimental data of Vizcaino *et al.* [12]. Solid curve: complex Kohn calculations. Broken curve: theoretical results of Gianturco and Lucchese [14]. Differential cross sections are in units of 10^{-16} cm^2/sr and energies are in eV.

tionally excited and dissociative attachment channels. This is consistent with the measurements of Allan, who estimates the total inelasticity (at 135° and not including DEA) at 2.0 eV to be about one-half of the elastic cross section. Our fixed-nuclei calculations, on the other hand, do not take explicit account of the vibrationally inelastic channels and the theoretical cross sections should therefore be identified with vibrationally summed quantities.

Also of interest is the sharp rise in the MTCS below 2.0 eV. The interpretation of this behavior is complicated by the fact that formic acid has a relatively large dipole moment, which undoubtedly contributes to the large cross sections at low energies; but in our earlier study, we also argued for the existence of a virtual state of A' symmetry, which would also exert a strong influence on the low-energy behavior of the cross sections. Unfortunately, the polar nature of the target precludes the use of a simple effective range analysis to accurately locate the position of a virtual state. Theoretical evidence for a virtual state comes from the fact that the cross section at low energies does not scale with the square of the target dipole moment D [25], as it would if the dipole interaction alone were responsible for this behavior. We can demonstrate that this is *not* the case with the data shown in Fig. 2, which shows the low energy behavior of the total cross section, computed using only the variationally determined T-matrix elements, for three different fixed-nuclei target geometries. The cross section at equilibrium geometry, where the target dipole moment is (in atomic units) −0.678, is shown along with two other geometries near the conical intersection discussed in [15], where the A' anion is barely bound and barely unbound relative to neutral formic acid. The dipole moments for the latter cases are −0.428 and −0.433, respectively. It is clear that the magnitude of the dipole moment does not explain the low energy behavior of the cross section in these cases. On the other hand, when the scattering is dominated by a virtual state, in which case there is a pole in the T-matrix on the negative imaginary k-axis close to the origin, the cross section at low energies will be large and sensitive to the precise location of the pole, which varies with geometry.

Turning to the differential scattering cross sections, Fig. 3 shows a comparison of our theoretical results with Allan's [11] low energy measurements of the elastic cross section at 135°. Apart from the resonance behavior in the vicinity of 2.0 eV, which we have already commented on above, the agreement is rather good. The notion that formic acid has a virtual state is reinforced by this comparison, since the rapid rise in the fixed-angle cross sections below ≈0.3 eV is seen in both theory and experiment. Indeed, Allan's measurements were deliberately taken at 135° to reduce the amount of di-

rect dipole excitation. The broad minimum in the cross section near 4.0 eV is also seen to be reproduced by the calculations.

Figure 4 shows our calculated angular differential cross sections at several energies in the resonance region. These are compared with the experimental data of Vizcaino *et al.* [12] which were measured at 1.8 eV. We note that the magnitude and shape of our calculated cross sections vary rapidly at scattering angles larger than 60°, which is consistent with the behavior of the calculated MTCS. We also note that the calculated DCS at 1.6 eV agrees rather well with the values measured at 1.8 eV, but given the sensitivity of the fixed-nuclei cross sections to energy in this region, the agreement should be regarded as somewhat fortuitous.

The agreement between the calculated DCS and the measured values of Vizcaino *et al.* improves markedly at energies above the resonance region, as seen in the comparisons presented in Fig. 5. Theory and experiment at 5.0, 10.0, and 15.0 eV agree in both magnitude and shape; in particular, we find that the minima seen in the measured cross sections near 100° are reproduced by the calculations. There is also reasonably good agreement between our results and the recent calculations of Gianturco and Lucchese [14], which were obtained from a single-center expansion using a static-exchange plus local polarization model. These authors also employed a dipole-Born correction in calculating their differential cross section which is similar to the procedure we have used. We note that their cross sections are smaller than our results at large scattering angles ($>100°$) and that the differences increase with energy.

IV. SUMMARY

We have presented the results of a theoretical study of elastic electron scattering from formic acid at low incident electron energies (0.1–10 eV). We performed fixed-nuclei calculations employing the complex Kohn method and determined the low order partial-wave components of the T-matrix variationally. Due to the polar nature of formic acid, we included the high order partial wave components of the T-matrix in the Born approximation via a closure formula, which allowed us to extract meaningful momentum transfer and differential cross sections. We have noted that, while the fixed-nuclei calculations show a sharp π^* shape resonance near 1.9 eV, which previous theoretical and experimental work has shown couples strongly to vibrational excitation and DEA, the recent experiments of Vizcaino *et al.* [12] and of Allan [11] suggest that this resonance is not prominent in vibrationally elastic scattering. Finally, we have argued that the extremely low-energy behavior of the cross section is indicative of a virtual state, which is also consistent with Allan's recent experiments.

ACKNOWLEDGMENTS

Work at the University of California Lawrence Berkeley National Laboratory was performed under the auspices of the US Department of Energy under Contract No. DE-AC02-05CH11231 and was supported by the U.S. DOE Office of Basic Energy Sciences, Division of Chemical Sciences. A.E.O. also acknowledges support from the National Science Foundation (Grant No. PHY-02-44911).

[1] L. Sanche, Eur. Phys. J. D **35**, 367 (2005).
[2] B. Boudaïffa, P. Cloutier, D. Hunting, M. A. Huels, and L. Sanche, Science **287**, 1658 (2000).
[3] J. Ellder *et al.*, Astrophys. J. **242**, L93 (1980).
[4] W. M. Irvive *et al.*, Astrophys. J. **342**, 871 (1989).
[5] A. Pelc, W. Sailer, P. Scheier, N. J. Mason, E. Illenberger, and T. D. Märk, Vacuum **70**, 429 (2003).
[6] A. Pelc, W. Sailer, P. Scheier, N. J. Mason, and T. D. Märk, Eur. Phys. J. D **20**, 441 (2002).
[7] A. Pelc, W. Sailer, P. Scheier, M. Probst, N. J. Mason, E. Illenberger, and T. D. Märk, Chem. Phys. Lett. **361**, 277 (2002b).
[8] M. Tronc, M. Allan, and F. Edard, in *Abstracts of Contributed Papers, XV ICPEAC, Brighton* (North Holland, Amsterdam, 1987).
[9] K. Aflatooni, B. Hitt, G. A. Gallup, and P. D. Burrow, J. Chem. Phys. **115**, 6489 (2001).
[10] V. Vizcaino, M. Jelisavcic, J. Sullivan, and S. J. Buckman, Bull. Am. Phys. Soc. **50**, 37 (2005).
[11] M. Allan, J. Phys. B **39**, 2939 (2006).
[12] V. Vizcaino, M. Jelisavcic, J. P. Sullivan, and S. J. Buckman, New J. Phys. **8**, 85 (2006).
[13] F. A. Gianturco and R. R. Lucchese, New J. Phys. **6**, 66 (2004).
[14] F. A. Gianturco and R. R. Lucchese, Eur. Phys. J. D **39**, 399 (2006).
[15] T. N. Rescigno, C. S. Trevisan, and A. E. Orel, Phys. Rev. Lett. **96**, 213201 (2006).
[16] T. N. Rescigno, C. W. McCurdy, A. E. Orel, and B. H. Lengsfield, *Computational Methods for Electron-Molecule Collisions*, edited by W. M. Huo and F. A. Gianturco (Plenum, New York, 1995).
[17] T. N. Rescigno, B. H. Lengsfield, and C. W. McCurdy, *Modern Electronic Structure Theory*, Vol. 1, edited by D. R. Yarkony (World Scientific, Singapore, 1995).
[18] T. H. Dunning, J. Chem. Phys. **53**, 2823 (1970).
[19] W. H. Hocking, Z. Naturforsch. A **31**, 1113 (1976).
[20] C. S. Trevisan, A. E. Orel, and T. N. Rescigno, Phys. Rev. A **68**, 062707 (2003).
[21] C. S. Trevisan, A. E. Orel, and T. N. Rescigno, Phys. Rev. A **70**, 012704 (2004).
[22] W. J. Hunt and W. A. Goddard, Chem. Phys. Lett. **3**, 414 (1969).
[23] T. N. Rescigno, B. H. Lengsfield, C. W. McCurdy, and S. D. Parker, Phys. Rev. A **45**, 7800 (1992).
[24] T. N. Rescigno and B. H. Lengsfield, Z. Phys. D: At., Mol. Clusters **24**, 117 (1992).
[25] W. R. Garrett, Mol. Phys. **24**, 465 (1972).